

**Sami El Khatib** 

Lebanese International University, Bekaa Campus, Khiyara, Lebanon

# Superficial bladder cancer diagnosis — the deliberate choice between fluorescent diagnosis and optical biopsy

## Address for correspondence:

Associate Professor Sami El Khatib (Msc, PhD)  
 Lebanese International University, Bekaa  
 Campus, 1108 Khiyara, Lebanon  
 E-mail: sami.khatib@liu.edu.lb

## ABSTRACT

Bladder carcinoma *in situ* (CIS) is a potentially invasive tumor whose early detection is a key step to ensuring the preservation of the bladder, reducing mortality, and improving the quality of patients' life. The early diagnosis of bladder cancer requires a sensitive technique that can detect the lesion to determine its stage and grade. ALA induced-PpIX makes it possible to detect tumors with 90% sensitivity. ALA hexyl ester (hALA) increases the sensitivity to 95%. Macroscopic techniques require a histological biopsy to define the tumor invasiveness. Imaging with Fibered Optic Confocal Fluorescence Microscopy allows the optical sectioning of examined tissues providing images with subcellular resolution after labeling with adequate fluorescent dye chosen based on the sensitivity of the used device. Available fluorescent agents are compatible with used devices; however, their toxicity and mutagenesis studies are unsatisfactory. During imaging, an optical fiber is introduced into the bladder via the urethra and placed in contact with the bladder wall. The distinction between the different types of epithelial cells is based on the cell size, morphology, and signal intensity. Although not fully adopted for clinical application, the FOCM represents a real asset that reduces invasiveness and complements the fluorescence-based endoscopy.

**Key words:** bladder cancer, photodiagnosis, optical biopsy, hexaminolevulinate, confocal microscopy

Oncology in Clinical Practice  
 DOI: 10.5603/OCP.2022.0027  
 Copyright © 2022 Via Medica  
 ISSN 2450–1654  
 e-ISSN 2450–6478

Oncol Clin Pract 2022; 18, 4: 263–274

## Bladder cancer

### Bladder histology

In mammals, the bladder wall is composed of four layers: the mucosal membrane, the submucosa, the muscular, and the serous layer. The mucosa consists of an epithelium known as urothelium [1], which consists of three types of epithelial cells: basal, intermediate, and superficial [2, 3]. The mucosa is separated from the sub-mucosa by a thin basal membrane, rich in laminin and collagen IV, whose integrity determines the invasive

potential of superficial bladder tumors [4]. The basal membrane is surrounded by a connective tissue called *lamina propria*. It contains capillary plexuses, blood vessels, and some smooth muscle fibers that form the *mucosal muscularis* [2, 3]. The detrusor muscle is usually composed of three layers of smooth muscle fibers separated by connective tissue. It is surrounded by perivesical fibro-adipose tissue that forms the serous layer [2, 5].

At the epithelium, the basal cells (10–20  $\mu\text{m}$ ) can be cubic or cylindrical and rest on the basal membrane. Their cytoplasm is basophilic, mitoses are only rarely encountered. Intermediate cells (15–50  $\mu\text{m}$ ) are oc-

Received: 13.03.2022    Accepted: 01.06.2022    Early publication date: 03.08.2022

This article is available in open access under Creative Common Attribution-Non-Commercial-No Derivatives 4.0 International (CC BY-NC-ND 4.0) license, allowing to download articles and share them with others as long as they credit the authors and the publisher, but without permission to change them in any way or use them commercially.

asionally attached to the basal blade but lose their cellular connections to the basal membrane during their maturation to replace superficial cells [3]. Their cytoplasm is less basophilic than that of basal cells and they are attached to adjacent cells by desmosomes. The superficial cells are the largest (20–100  $\mu\text{m}$ ), covering the surface of the epithelium. Their cytoplasm is less basophilic and contains large lysosomes. These three types of cells have a profile that evolves from small undifferentiated basal cells through intermediate cells to highly differentiated superficial cells. In humans, urothelium consists of 3 to 6 cell layers. In rats, the number of layers is limited to 3 [2, 3].

### Epidemiology and etiology

In 2005, the American Cancer Society estimated the number of people with bladder cancer in the United States at 63 210, including 47010 men and 16200 women. The estimated number of deaths from bladder cancer is 13180, including 8970 men and 4210 women. In terms of incidence, bladder cancer ranks fourth in men (7% of cases) and ninth in women (2% of cases). Mortality from bladder cancer is 3% in men and less than 1% in women [6].

Tobacco poisoning is the primary risk factor for bladder tumor induction [7]. Exposure to certain derivatives of industrial products, including derivatives of aromatic amines (naphthylamine, xenylamine, benzidine) increases the risk of developing bladder tumors [8], as well as exposure to cyclophosphamide [9]. Urinary tract infection and chronic bladder irritation (probe and stones) promote the development of transitional bladder carcinomas [10]. Urinary bilharzia, a trematode-related parasitic infection of the genus *Schistosoma*, is a known risk factor for bladder epidermis cancer, particularly in Egypt [11]. One of the most commonly found genetic mutations is the p53 gene on chromosome 17 [12].

### TNM classification of bladder tumors

Bladder tumors are classified as epithelial (transitional carcinomas, squamous cell carcinomas) and non-epithelial (sarcoma, metastasis) tumors. The majority of tumors are epithelial and transitional carcinomas accounting for 90% of bladder tumors [13]. The prognosis of bladder tumors depends on several parameters including (1) the stage or degree of invasion, (2) the grade or degree of cell differentiation, (3) the appearance of vascular or lymphatic invasion, and (4) the presence of carcinoma *in situ* (CIS) [14].

Among transitional carcinomas, 70% are superficial carcinomas (Ta, T1, CIS) and 30% are invasive tumors (T2, T3, and T4) [14]. The WHO classification divides transitional carcinomas into three grades (I, II, and III) according to their degree of cell differentiation. Grade I is the most differentiated and prognostic, and Grade III is the least differentiated and has a poor prognosis [13, 15]. Within 24 months of diagnosis, the rate of progression to an invasive tumor is 2%, 11%, and 45% for grade I, II, and III tumors, respectively [15]. The presence of *in situ* carcinoma (CIS) is associated with a high risk of progression to an invasive tumor that invades the muscle layer of the bladder wall [16, 17] or adjacent organs, such as the prostate, vagina, or rectum. Tumor cells can also colonize blood and lymphatic vessels, inducing regional, general, and other organ metastases [18, 19].

### Superficial bladder tumors

Superficial transitional carcinomas include stage Ta, T1, and carcinoma *in situ*. Stage Ta tumors account for nearly 70% of superficial tumors [20]. These papillary lesions are confined exclusively to the mucosa and the basal membrane remains intact (Fig. 1). Stage Ta tumors are associated with a recidivism rate of 50–75% and a low rate of progression (< 5%) [14]. TaGI stage

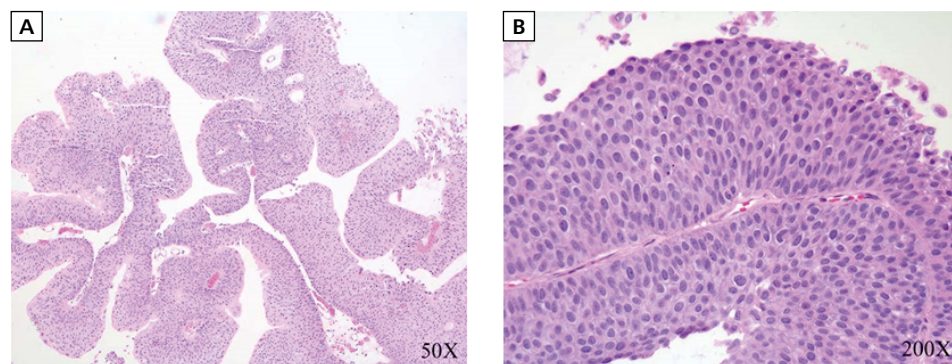


**Figure 1A.** Papillary transitional carcinoma; **B.** Papillary lesion with thickening of the epithelium without alteration of cell polarity, cellular atypia is weak or non-existent, mitosis is rare

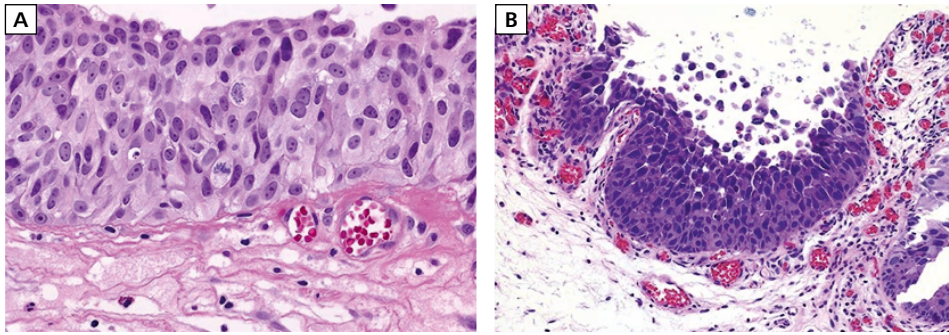


**Figure 2A.** Carcinoma *in situ* (CIS), cells are oriented anarchically, cytoplasm abundant with an irregular nucleus, abundant mitoses; **B.** Loss of cohesion and detachment of cells with completely bare areas in a CIS

tumors rarely progress (2%), followed by TaGII stage tumors (6%), while TaGIII stage tumors progress in 48% of cases [15]. Stage T1 tumors are papillary or nodular tumors marked by *lamina propria* invasion, but the musculoskeletal gland remains intact. The rate of progression of T1GII and T1GIII tumors is in the region of 21% and 48% respectively, while T1GI rarely progresses [15, 20].

Carcinoma *in situ* (CIS) was first described by Melicow in 1952 [21]. CIS is a flat tumor lesion limited to the epithelium. In the majority of cases (90%), CIS is associated with other invasive transitional carcinomas that are diagnosed concomitantly or prior to CIS [22, 23]. Histologically, CIS is characterized by obvious cytological abnormalities corresponding to high-grade dysplasia G III [23]. The CIS is marked by major cellular disorganization with a loss of nuclear polarity and a lack of cell cohesion. The nuclei are voluminous, of uneven size, and are characterized by hyperchromatic and large nucleoli. Mitoses are numerous and visible in all cell layers; the chorion is inflammatory and hypervascularized. Due to a lack of cell cohesion, which leads to excessive desquamation of the normal urothelium, the chorion is almost naked in some areas (Fig. 2) [23, 24]. This explains the sensitivity of cytological examination in the context of CIS, which reaches 90% with a specificity of 98% [20]. CIS is known to be the precursor of invasive tumors [25] with a risk of progression of the order of 36–83% [16, 26]. The average time between diagnosis and development of an invasive tumor is about 5 years [27]. In a study of 62 patients with carcinoma *in situ*, Utz et al. [23] showed that 82% of patients treated with transurethral resection relapsed over a 5-year period. Seventy-three percent of patients develop invasive carcinoma, and 65% die from complications of bladder cancer [23].

Transurethral resection associated with chemotherapy or immunotherapy (BCG) is the treatment of choice for superficial tumors. For CIS, the standard treatment is an intravesical instillation of BCG over a 6-week period [28]. If urinary cytology and biopsy results are positive,

a second cycle of 6 weeks of BCG treatment is indicated. If positive cytology persists after the second cycle, total cystectomy is indicated [28].

Early detection of carcinoma *in situ* is, therefore, an essential step in ensuring bladder preservation, reducing mortality from bladder cancer, and improving the quality of life of patients. In recent years, efforts have been made to search for new diagnostic and therapeutic techniques capable of detecting CIS lesions and achieving their eradication.

### Fluorescence diagnosis of bladder cancer

Urine cytology, conventional white light cystoscopy, and random tissue biopsy are the main techniques applied for the diagnosis of bladder cancer. Carcinoma *in situ* (CIS) is an aggressive lesion, its presence at the epithelium is associated with a high risk of progression ranging from 36 to 83% [16, 26, 29]. Urine cytology is perceived as a non-invasive diagnostic technique. It is sensitive to the presence of high-grade tumors detected in 79% of cases but is less sensitive to the presence of low-grade tumors detected in 26% of the cases [30]. Due to the absence of architectural anomalies, the ability of conventional cystoscopy to properly detect carcinoma *in situ* is low, its sensitivity is of the order of 41%, and most lesions go undetected during the examination [31]. In the case of positive cytology and negative cystoscopy, a random biopsy is recommended. However, CIS lesions go undetected in more than 90% of cases [32]. The presence of CIS is not the only cause of recurrence and progression of bladder cancer. Incomplete resection of tumors is an essential source of relapse. In a series of 150 patients, 75% of cases show non-invasive residual tumors at the time of a second transurethral resection, and 29% of cases progress to invasive tumors [33]. A more sensitive technique compared to conventional cystoscopy is needed to locate tumor lesions and guide

the practitioner in resection of these lesions to reduce the risk of recurrence and avoid the risk of progression [34]. The combination of the cystoscopy technique with the fluorescence phenomenon is an important advance in the field of bladder cancer diagnosis. However, discrepancies and variations in the type and the quality of the used endoscopic apparatus affect the management outcomes in photodiagnosis-assisted resection [35].

#### History of fluorescence diagnosis

The first observation of fluorescence of porphyrins from tumor lesions was reported by Policard in 1924 [36]. He found that experimental rat tumors emitted red fluorescence during light excitation. This was attributed to endogenous porphyrins synthesized by tumor colonizing bacteria. In 1942, Auler and Banzer [37] were the first to observe the accumulation of exogenous porphyrins in the tumor. They noted that hematoporphyrin injected into the rat accumulated in tumor lesions and lymph nodes. In 1948, Figge et al. [38] demonstrated that many porphyrins had a selective affinity not only for tumors but also for embryonic and traumatized tissues in rats. In 1961, Lipson et al. [39] introduced the use of the hematoporphyrin derivative (HpD) in the detection of transplanted tumors in mice.

In 1976, Kelly and Snell [40] were the first to introduce fluorescence detection of bladder tumors 24 hours after intravenous injection of hematoporphyrin (Hp) at 2 mg/kg. The cystectomy pieces observed under UV light showed that the tumor areas emitted red fluorescence while the normal mucous membranes did not fluoresce. In 1982, Benson [41] described fluorescence detection of carcinoma *in situ* 2 hours after intravenous injection of 2.5 mg/kg HpD in humans. Intravesical instillation of porphyrins in rats led to the accumulation of photosensitizer, detected by fluorescence at the vesical wall, by sparing other organs [42]. However, it is associated with a loss of selectivity between the normal epithelium and the tumor [43]. Leveckis [44] was the first to describe intravesical instillation of aminolevulinic acid (ALA) in the rat's healthy bladder but was unable to detect PpIX. It was subsequently shown that sufficient synthesis for the detection of PpIX by fluorescence in rats requires instillation of ALA concentrations above 200 mg/mL for at least 2 hours [34, 45]. Intravesical instillation of ALA in a bladder tumor model in rats leads to epithelial synthesis of PpIX, but no selectivity between normal epithelium and tumor epithelium [43, 46]. On the other hand, intravesical instillation of ALA in humans leads to more selective synthesis of PpIX in tumor lesions, making it possible to detect CIS with sensitivity greater than 90% [47–51].

Kloek et al. [52, 53] synthesized a series of ALA esters, including ALA hexylester (hALA), which presents

a compromise between water solubility and lipophilicity. Intravesical instillation of ALA hexylester increases the amount of synthesized PpIX produced for 1 to 2 hours with a 20-fold lower hALA concentration [54, 55]. In 1999, Marti et al. [55] reported the first clinical study using intravesical instillation of hALA. To improve diagnostic specificity, D'Hallewin et al. [56, 57] propose intravesical instillation of hypericin (hydroxylated phenanthro-perylenequinone), a fluorescent pigment synthesized by plants of the genus *Hypericum*, including *Hypericum perforatum* [58].

#### Place of fluorescence diagnosis in bladder cancer

The principle of fluorescence diagnosis is based on the interaction of light with a chromophore that accumulates selectively in the tumor. The identification of tumor lesions is based on the difference in intensity of fluorescence emitted by healthy tissue and tumor tissue. Chromophores can be endogenous (Autofluorescence) or exogenous (photosensitizer) [59]. When excited by blue or violet light (375–440 nm), the photosensitizer emits fluorescence in the red region. The use of a high-pass filter (> 520 nm) makes it possible to visualize areas containing high concentrations of the photosensitizer. The three molecules used in clinical studies are ALA, hALA, and hypericin.

### Endogenous fluorophores

Autofluorescence is the fluorescence of endogenous tissue chromophores. It can be used to obtain diagnostic information from the tissue. Alfano et al. [60] were the first to describe *in vitro* endogenous fluorescence diagnosis. The main endogenous chromophores that contribute to tissue autofluorescence of the bladder are tryptophan, collagen, and the reduced form of dinucleotide nicotinamide (NADH) [61–63]. Autofluorescence spectra acquired through an optical fiber placed in contact with the wall exhibit a decrease in the fluorescence intensity of the tumors compared to the normal epithelium [61, 64–66]. The reduction in the fluorescence intensity of the tumor may be due to increased blood uptake, low NADH, and thickening of the epithelium [61, 66]. Thus, the autofluorescence signal for carcinoma *in situ* is between that of the normal epithelium and that of papillary tumors [66–68]. Frimberger et al. [69] described an autofluorescence imaging system capable of detecting bladder tumors with 95% sensitivity and 42% specificity. The combination of the autofluorescence technique with the fluorescence technique after instillation of ALA increases the specificity of the ALA-PpIX technique by 20% [69].



## Exogenous fluorophores

There are two main approaches to the fluorescence diagnosis of exogenous fluorophores. An *in vivo* fluorescence cystoscopy approach and an *ex vivo* fluorescence cytology approach.

### Fluorescence cystoscopy

The results of the various clinical studies concerning the diagnosis of bladder CIS by fluorescence cystoscopy are shown in Table 1.

**ALA:** 3% ALA solution (180mM) is instilled in the bladder for 2 to 6 hours before cystoscopy. The sensitivity of the technique varies from 87% to 100% with an average value of 92.3%. The specificity of the technique varies from 51% to 68.5% with an average value of 62.9%. The technique detects an additional 30% to 50% of CIS compared to conventional cystoscopy [31, 47–50, 68, 70–72]. The relatively low specificity is due to the fluorescence of modified tissue areas, such as cystitis or hyperplasia, areas of anterior resection, or areas of inflammation following recent intravesical treatment, which limit the use of the technique for a period of 6 weeks to 6 months after the intervention [73, 74]. However, genetic analysis of false-positive areas of hyperplasia shows that some lesions exhibit chromosomal alterations comparable to those observed in papillary tumors [75]. Transurethral resection guided by fluorescence reduces by 40–50% the residual tumor rate after resection [71, 76].

**hALA:** A solution of hALA (Hexvix®) at a concentration of 8 mM is instilled in the bladder for 1 to 2 hours before the exam. The sensitivity of the technique varies from 92.2 to 97% with an average value of 95%. The specificity of the technique is of the order of 75.4%. The technique detects more than 90% of CIS [77, 78]. Compared to conventional cystoscopy, fluorescence cystoscopy with hALA detects 67% of additional CIS cases. Although intravesical instillation of ALA or hALA provides comparable results, the use of hALA is justified for several reasons; the reduction in instillation

time from 2–6 hours for ALA to 1–2 hours for hALA, the reduction of the concentration of the solution to be instilled by 180 mM (3%) for ALA at 8 mM (0.2%) (Reduction of factor 20), and the increase in the rate of PpIX synthesized by 22% after intravesical instillation for 4 hours in a row or by 110% after 2 hours of instillation followed by 2 hours of waiting [79, 80]. Recently, hALA has been shown to enable the detection of bladder cancer cells in liquid biopsies [81].

**Hypericin:** Hypericin solution is instilled in the bladder at a concentration of 8 $\mu$ M for 2–4 hours before the examination. The sensitivity of the technique varies from 82 to 94% with an average value of 90%. The specificity of the technique varies from 91 to 97% with an average value of 94.8%. The hypericin fluorescence cystoscopy technique is characterized by sensitivity comparable to that obtained with ALA or hALA, however, the specificity of this technique is greater than the last two (Tab. 2) [56, 57, 82].

### Fluorescence cytology

Fluorescence cytology involves combining urinary cytology with fluorescence diagnosis. Two different approaches are possible. The first involves intravesical instilling an ALA (3%) or hypericin (8 $\mu$ M) solution and microscopic examination of the sediments of the wash solution [83, 84]. The second approach involves incubating the cells recovered from the bladder wash with an *ex vivo* hypericin solution (15 min, ambient temperature) before performing the microscopic examination [85]. The sensitivity and specificity of fluorescence cytology after intravesical instillation of ALA (3%, 2–3 h) are estimated at 86% and 75% compared to 79% and 88%, respectively, for conventional cytology [84]. Pytel et al. [83] reported 98% sensitivity for fluorescence cytology after intravesical instillation of ALA (3%) or hypericin (8  $\mu$ M). Olivo et al. [85] found that cells recovered from urinary lavage and incubated in the presence of hypericin are considered malignant if they accumulate at a higher rate (8.5 times) than the baseline value established by healthy cells.

**Table 1. Comparison of fluorescence cystoscopy with conventional cystoscopy**

|                         | Sensitivity % | Specificity % | Benefits  | Disadvantages  |
|-------------------------|---------------|---------------|---|--|
| Conventional cystoscopy | 73            | 60            | Detection of papillary lesions<br>Reduced time and cost | Low sensitivity for CIS detection<br>Low specificity         |
| ALA                     | 92            | 62            | Improves the sensitivity of conventional cystoscopy     | Low fluorescence specificity on modified areas               |
| Hexvix®                 | 95            | 75            | Reduction of time and concentration of instillation     | Improved specificity compared to ALA, but still insufficient |
| Hypericin               | 90            | 94            | Improves fluorescence cystoscopy specificity            | Primary results to be confirmed in larger studies            |

ALA — aminolevulinic acid

**Table 2. Diagnosis of bladder carcinoma by aminolevulinic acid, aminolevulinic acid hexylester, and hypericine induced fluorescence**

|                     | Nb          | PS          | Concentration<br>Time (H) | Sensitivity<br>%   | Specificity<br>% | Supplemental fluorescence cystoscopy<br>(CF)/Conventional cystoscopy (CC)  |
|---------------------|-------------|-------------|---------------------------|--|------------------|--|
| (Kriegmair, 1994)   | 68          | ALA         | 3%<br>3/5                 | 100  | 68.5             | 32.5%  |
| (Kriegmair, 1996)   | 104         | ALA         | 3%<br>2/3                 | 96.9   | 66.6             | 20%  |
| (Jichlinski, 1997)  | 34          | ALA         | 3%<br>6/7                 | 89   | 56               | 40%  |
| (Jichlinski, 1997)  | 51          | ALA         | 3%<br>4/6                 | 93.3   | 51               | 27%  |
| (Jichlinski, 1997)  | 33          | ALA         | 3%<br>6/7                 | 82.9   | 81.3             | 32.5%  |
| (D'Hallewin, 1998)  | 16          | ALA         | 1, 2, 3%<br>3             | 94   | 54               | 97% of CIS cases detected by CF compared to 34% detected by CC   |
| (Koenig, 1999)      | 55          | ALA         | 3%<br>2/3                 | 87   | 59               | 20% CIS  |
| (Kriegmair, 1999)   | 208         | ALA         | 3%<br>2.8 h               | 96   | 65               | CF detects 82 (25%) additional cases<br>31% belong to non-specific or normal epithelium                                      |
| (Dominicis, 2001)   | 49          | ALA         | 3%<br>2/3                 | 87   | 63               | 30%  |
| (Zaak, 2001)        | 605         | ALA         | 3%<br>2 h 30              | 97   | 65               | 34.2% invisible per CC<br>56.8% additional CIS   |
| (Filbeck, 2002)     | 279         | ALA         | 3%<br>2/3                 | 17 cases of CIS (57%) and 7 cases of Dys (44%) are detected by CF<br>57% additional detection rate for CIS and Dys |                  |  |
| (Zaak, 2002)        | 713         | ALA         | 3%<br>2/3                 | 91.1% of CIS detected by CF compared to 47.2 per CC<br>80.6% of Dys are detected by CF compared to 69% by CC       |                  |  |
| <b>TOTAL</b>        | <b>2215</b> | <b>ALA</b>  | <b>3%<br/>2–6</b>         | <b>92.3</b>  | <b>62.9</b>      | <b>CF<sub>ALA</sub> allows detection of 20–50% additional CIS/CC</b>   |
| (Lange, 1999)       | 25          | hALA        | 4, 8, 16 mM<br>2 + 2      | 92.2   | 71.8             | Optimum concentration 8 mM<br>2 hours instillation + 2 hours waiting   |
| (Jichlinski, 2003)  | 52          | hALA        | 8 mM<br>1h                | 96   | 79               | 47 lesions detected by hALA alone<br>12 / 13 (92.3%) CIS detected by hALA<br>CF detects 10 times more CIS/CC                 |
| (Schmidbauer, 2004) | 286         | hALA        | 8 mM<br>1h                | 97   | –                | CF detects 67% more CIS/CC<br>and 28% more patients with CIS<br>FC vs. CC (CIS): 97% vs. 58%<br>FC vs. CC:(Dys): 94% vs. 53% |
| <b>TOTAL</b>        | <b>363</b>  | <b>hALA</b> | <b>8 mM<br/>1 h</b>       | <b>95</b>  | <b>75.4</b>      | <b>CF hALA allows detection of more than 90% CIS<br/>CF hALA allows detection of 67% CIS suppl./CC</b>                       |
| (D'Hallewin, 2000)  | 40          | Hyp         | 8 μM<br>2–4               | 93   | 98.5             | No false positives<br>Contact time comparable to ALA at 8μM  |
| (D'Hallewin, 2002)  | 87          | Hyp         | 8 μM<br>2–4               | 94   | 95               | No photobleaching during examination<br>or resection   |
| (Sim, 2005)         | 41          | Hyp         | 8 μM<br>2–4               | 82   | 91               | Additional detection of 29% tumours  |
| <b>TOTAL</b>        | <b>168</b>  | <b>Hyp</b>  | <b>8 μM<br/>2–4</b>       | <b>90</b>  | <b>94.8</b>      | <b>CF Hyp improves detection specificity CF Hyp allows detection of 29% additional cases/CC</b>                              |

ALA — aminolevulinic acid; CC — conventional cystoscopy; CF — fluorescence cystoscopy; CIS — carcinoma *in situ*; hALA — aminolevulinic acid hexylester; Hyp — hypericine induced fluorescence; Nb — number; PS — photosensitizing

## Confocal microscopy

### Optical biopsy

The diagnosis of bladder cancer requires using a technique that provides the following information: (i) the location in the epithelium (detection), (ii) the degree of wall invasion (tumor stage), (iii) and histological differentiation (cell grade) [86]. For several years, efforts have been focused on the development of optical biopsy techniques. The principle of these techniques is based on the interaction of light and tissues. The term optical biopsy encompasses various methods which use the properties of light to instantly retrieve diagnostic information and which are compatible with endoscopy [87, 88].

Optical biopsy techniques under development include spectroscopic methods and optical imaging methods:

**Spectroscopic methods** include, among others, the technique of elastic scattering spectroscopy (ESS) [86, 89, 90], the technique of non-elastic scattering spectroscopy (Raman effect spectroscopy) [91], and fluorescence spectroscopy (LIFS, light induced fluorescence spectroscopy) [61, 65, 92].

**Optical imaging methods** include the optical coherence tomography technique (OCT) [93–96] and the fiber optic confocal microscopy technique (FOCI) [97, 98].

Among the optical biopsy techniques, fiber confocal microscopy could be a tool capable of visualizing, *in vivo* and *in situ*, the histology of the observed tissue, without resorting to the sampling of biological material. This technique consists in coupling a confocal microscopy system to an optical fiber making it possible to perform confocal imaging, *in vivo*, by endoscopic route [99].

### Principle of confocal microscopy

One of the major problems of classical epi-fluorescence microscopy is the presence of a significant background noise linked to the thickness of the object observed. Although the focusing is done on a precise focal plane, the information recording is marred by background noise that is superimposed on the image of the observed plane: this noise results from the excitation by the source light of fluorochromes located on the light path [100].

The confocal microscope acts like an optical microtome. Its principle consists in focusing the beam of the excitation light on a point of the sample and recovering only the light signal emitted by this same point. The signal passes through the aperture of a diaphragm for both illumination and detection paths. The role of the illumination diaphragm is to limit the illumination zone to a single point of the sample examined. The detection diaphragm blocks light from adjacent planes on either side of the focal plane. The two diaphragms are projected by a lens on the same point of the sample to make them confocal [97]. The 2D image is constructed point by point by the scanning (X, Y) of the field of view. The optical sectioning of successive focal planes (Z) allows a 3D reconstruction of the tissue volume. The combination of high spatial resolution with the ability to perform optical sectioning through confocal imaging results in the acquisition of high-resolution subcellular images extended to several tens of  $\mu\text{m}$  thick. Confocal microscopy provides a means of visualizing cell and nuclear size and arrangement, as well as tissue structures (vessels, capillaries), with or without the addition of contrast agents [97, 101].

### Fiber optic confocal microscopy

The confocal microscope is made up of two distinct entities: a mechanical part and an optical part. The mechanical part comprises the light source, detection system, and scanning system. The optical part corresponds to the objective. Fiber confocal microscopy consists of separating the mechanical entity from the optical scope by means of an optical fiber formed of a bundle of flexible fibers which ensure the transfer of the excitation light from the source to the tissue. These fibers recover information from the fabric on return. The objective incorporated in the head of the optical fiber makes it possible to access the imaging of organs *in vivo* by endoscopy and bypass the bulk generated by the confocal microscope [97, 102]. There are two imaging modalities used in fiber confocal microscopy: confocal reflectance imaging and confocal fluorescence imaging. The resolution of these imaging techniques is shown in Table 3.

**Table 3. Resolution parameters of the different confocal microscopy approaches**

| Confocal microscopy approach     | Montage  | Resolution<br>Lateral / axial            | Penetration<br>depth  | References      |
|----------------------------------|----------|--|-----------------------|-----------------|
| Confocal Reflectance Microscopy  | No Fiber | < 1 $\mu\text{m}$ /3 $\mu\text{m}$       | 100–500 $\mu\text{m}$ | (Sokolov, 2002) |
|                                  | Fibred   | 2 $\mu\text{m}$ /6 $\mu\text{m}$         | 100–200 $\mu\text{m}$ | (Sokolov, 2002) |
| Confocal Fluorescence Microscopy | No Fiber | < 1 $\mu\text{m}$ /5 $\mu\text{m}$       | 200–500 $\mu\text{m}$ | (Koenig, 2003)  |
|                                  | Fibred   | 2,5–5 $\mu\text{m}$ /15–20 $\mu\text{m}$ | 0–80 $\mu\text{m}$    | (Laemmel, 2004) |

**Confocal reflectance imaging:** In reflectance mode, the excitation phenomenon and the emission phenomenon are produced at the same wavelength. Confocal reflectance imaging is based on the difference in back-scattering phenomena between nuclear and cytoplasmic compounds in the cell. These differences may be tissue specific or induced by an exogenous contrast agent (acetic acid) capable of modifying the optical properties of cellular compounds. It allows highlighting the difference between the nucleus and the other cytoplasmic compounds [97].

**Confocal fluorescence imaging:** In fluorescence mode, the technique requires the presence of a fluorescent molecule to visualize cellular compounds. This molecule can be endogenous (autofluorescence) or exogenous (fluorescent marker).

In autofluorescence, the images mainly come from native fluorophores often confined to connective tissue (collagen, flavins, elastins) [97].

In fluorescence, the images come from exogenous fluorophores which mark cellular compounds. Among the molecules used, there are nuclear markers such as Syto 17 [103] or Cresyl violet [104], membrane markers such as fluorescein [105], or antibodies coupled to a fluorescent substance such as FITC [106]. Nuclear markers should be used with caution because of their mutagenic potential when interacting with nuclear DNA.

## Cell ViZio™

### System description

Cell viZio™ is a confocal imaging instrument, developed by the French company Mauna Kea Technologies [107]. Cell viZio™ is intended for non-invasive *in situ* and *in vivo* imaging thanks to the coupling to a miniaturized optical fiber, compatible with endoscopy [80, 108]. The system is composed of (i) an optoelectronic box containing a laser diode (488 nm) as an excitation source, (ii) an optical fiber (iii), and a control, recording, and processing system computer image [98]. Optical fibers represent for Cell viZio™ the equivalent of an objective for a microscope [107].

### Image training and processing

The excitation source consists of a solid 488 nm laser diode compatible with most markers used *in vivo*. The confocal nature of the system is due to the size of the core of each fiber in the bundle. Indeed, the diameter of 2 $\mu$ m serves as excitation and then detection diaphragm and gives the system its confocal character [109]. The excitation light is focused on the tissue through a micro-objective located at the distal level of the fiber.

The illuminated spot excites the fluorophore located at a specific distance in the tissue. Excitation light is sequentially injected into each fiber producing a parallel illumination beam. This is then separated by a dichroic mirror in order to separate the excitation channel from the detection channel. The beam is then deflected angularly in two spatial directions by a scanning system (X, Y) then injected point by point for a given line and line after line to constitute a 2-dimensional image. The spot illuminating the tissue is backscattered following the reverse path of the incident beam to a detection system. The detected signal is digitized for viewing on the screen. Twelve frames per second can be acquired to capture real-time video footage. The raw information at the output of the detector is processed by an algorithm so that it can be viewed and then interpreted [98].

### Applications of confocal microscopy

Fiber confocal imaging could be useful for a large number of medical applications, including the early diagnosis of epithelial cancers, especially those at high risk of recurrence and progression [97]. The fields of application of confocal microscopy are wide, they relate in particular to skin [105, 106], gastrointestinal [110], oral [111, 112] lesions, as well as the bladder [80] and cervix [113]. Experience with confocal microscopy in bladder imaging is still very limited. Koenig et al., evaluated the potential of confocal laser scanning microscopy (CLSM or Confocal Laser Scanning Microscopy) in imaging the rat bladder wall *in vivo* after laparotomy, without staining the tissue. The images are obtained in the near infrared at 1064 nm allowing the imaging of structures at a maximum depth of 300  $\mu$ m, with an axial resolution of 0.5 to 1  $\mu$ m and a lateral resolution of 3 to 5  $\mu$ m. The CLSM allows imaging of the normal rat bladder epithelium. Epithelial cells, lamina propria, collagen fibers, muscle fibers, capillary plexuses, and blood vessels are easily visualized [103]. In a second *ex vivo* study, Koenig et al. evaluated the potential of confocal fluorescence microscopy after intravesical instillation of a fluorescent nucleic marker (Syto 17). Imaging is performed with a standard laser scanning confocal microscope (Zeiss LSM 410). Two hours after instillation of a solution of Syto 17 (10  $\mu$ M), the rats are euthanized. The bladders are removed and examined under the confocal microscope on sections 3 to 5  $\mu$ m thick with a lateral resolution of 0.5 to 1  $\mu$ m. Confocal fluorescence microscopy made it possible to distinguish different types of cells of the epithelium (superficial, intermediate, and basal) and the lamina propria. Cell structures and characteristics (shape, size, chromatic profile, nucleoli, mitosis, and nucleocytoplasmic relationship) can be distinguished. On deep cuts, connective tissue structures (collagen fibers, vessels, capillary plexuses, erythrocytes) can be observed [103, 109, 112].



## Clinical assessment of real-time confocal endo-microscopy in the diagnosis of bladder carcinoma

Confocal Laser Microscopy has been introduced to the endoscopic clinical practices in the framework of asserting the diagnosis of the potential bladder malignancies. The validation of this technique has been based on high-resolution endoscopic optical images, which enable clinicians to establish a categorical tumor grading during cystoscopy. In the study conducted by Liem et al. [114] confocal laser endomicroscopy (CLE) has been shown to be a valuable modality able to identify and ensure a real-time tumor grading of the urothelial lesions although superficial neoplasms still represent an unmet challenge. Marien et al. [115] coupled the confocal laser endomicroscopy with two fluorophores, namely the fluorescein and the PpIX inducing prodrug hexyl aminolevulinate (HAL), to adopt the cytological and histological criteria of bladder cancer diagnosis in patients eligible for HAL-PpIX assisted transurethral resection. Biopsies were examined using either confocal laser microscopy or Cell Vizio (488; 660 nm dual system). Real-time confocal microscopy showed promising potential in cytodetection ability and subcellular visualization of the nucleocytoplasmic abnormalities associated with neoplastic cellular features [115]. In this context, Cell Vizio mediated endomicroscopy has been considered a quantum leap in the selection of patients eligible for conservative tumor management [107]. When combined with white light cystoscopy, confocal fluorescence video microscopy, performed after intravesical instillation with fluorescein, showed a high consistency correlated with conventional histopathological classification in 85.7% of low-grade and 80% of high-grade urothelial lesions [99].

## Conclusions

The technological transition from conventional endoscopy of the bladder to the fluorescence cystoscopy after intravesical instillation with photosensitizers or PpIX-induced prodrugs (ALA and h-ALA) associated with blue-light imaging systems has improved the sensitivity of papillary and superficial bladder cancer detection to a rate of 95% with Hexvix, but without offering further insights on the degree of invasiveness and malignancy. Fiber Optic Confocal Fluorescence endoscopy has been introduced to scan urological tumors by providing explicit images at the microscopic level showing the architectural landscape of urothelial cytology which will pave the road for a systematic follow-up of bladder tumors. The possibility of carrying out optical sectioning by the means of confocal imaging through an

optical fiber compatible with endoscopy could make it possible to visualize different histological layers of the epithelium in a non-invasive manner, from the surface and up to several tens of  $\mu\text{m}$  deep. This progress holds the greatest potential, not only for mere detection of the epithelial lesions but also for providing real-time intraoperative histology with the ability to discern between normal and abnormal tissues, which helps in very accurate localization and cellular characterization of the epithelial tumors.

## Conflict of interest

None declared.

## References

- Melicow MM. Tumors of the Urinary Drainage Tract: Urothelial Tumors. *Journal of Urology*. 1945; 54(2): 186–193, doi: [10.1016/s0022-5347\(17\)70066-3](https://doi.org/10.1016/s0022-5347(17)70066-3).
- Hicks RM. The mammalian urinary bladder: an accommodating organ. *Biol Rev Camb Philos Soc*. 1975; 50(2): 215–246, doi: [10.1111/j.1469-185x.1975.tb01057.x](https://doi.org/10.1111/j.1469-185x.1975.tb01057.x), indexed in Pubmed: 1100129.
- Jost SP, Gosling JA, Dixon JS. The morphology of normal human bladder urothelium. *J Anat*. 1989; 167: 103–115, indexed in Pubmed: 2630525.
- Mostofi FK, Davis CJ. Epithelial abnormalities of urinary bladder. *Prog Clin Biol Res*. 1984; 162A: 81–93, indexed in Pubmed: 6483921.
- Mostofi FK, Sesterhenn IA. Pathology of epithelial tumors & carcinoma *in situ* of bladder. *Prog Clin Biol Res*. 1984; 162A: 55–74, indexed in Pubmed: 6091153.
- Jemal A, Murray T, Ward E, et al. Cancer statistics, 2005. *CA Cancer J Clin*. 2005; 55(1): 10–30, doi: [10.3322/canjclin.55.1.10](https://doi.org/10.3322/canjclin.55.1.10), indexed in Pubmed: 15661684.
- Clavel J, Cordier S, Boccon-Gibod L, et al. Tobacco and bladder cancer in males: increased risk for inhalers and smokers of black tobacco. *Int J Cancer*. 1989; 44(4): 605–610, doi: [10.1002/ijc.2910440408](https://doi.org/10.1002/ijc.2910440408), indexed in Pubmed: 2793232.
- Indulski JA, Lutz W. Biological monitoring of risk of bladder cancer in persons occupationally exposed to aromatic amines. *Pol J Occup Med Environ Health*. 1992; 5(2): 143–151, indexed in Pubmed: 1392660.
- Travis LB, Curtis RE, Boice JD, et al. Bladder cancer after chemotherapy for non-Hodgkin's lymphoma. *N Engl J Med*. 1989; 321(8): 544–545, doi: [10.1056/NEJM198908243210815](https://doi.org/10.1056/NEJM198908243210815), indexed in Pubmed: 2761594.
- West DA, Cummings JM, Longo WE, et al. Role of chronic catheterization in the development of bladder cancer in patients with spinal cord injury. *Urology*. 1999; 53(2): 292–297, doi: [10.1016/s0090-4295\(98\)00517-2](https://doi.org/10.1016/s0090-4295(98)00517-2), indexed in Pubmed: 9933042.
- Tricker AR, Mostafa MH, Spiegelhalter B, et al. Urinary excretion of nitrate, nitrite and N-nitroso compounds in Schistosomiasis and bilharzia bladder cancer patients. *Carcinogenesis*. 1989; 10(3): 547–552, doi: [10.1093/carcin/10.3.547](https://doi.org/10.1093/carcin/10.3.547), indexed in Pubmed: 2924399.
- Dalbagni G, Presti JC, Reuter VE, et al. Molecular genetic alterations of chromosome 17 and p53 nuclear overexpression in human bladder cancer. *Diagn Mol Pathol*. 1993; 2(1): 4–13, indexed in Pubmed: 7904525.
- Mostofi FK, Davis CJ, Sesterhenn IA, et al. Histological Typing of Urinary Bladder Tumours. 1999, doi: [10.1007/978-3-642-59871-5](https://doi.org/10.1007/978-3-642-59871-5).
- Lee R, Droller MJ. The natural history of bladder cancer. Implications for therapy. *Urol Clin North Am*. 2000; 27(1): 1–13, vii, doi: [10.1016/s0094-0143\(05\)70229-9](https://doi.org/10.1016/s0094-0143(05)70229-9), indexed in Pubmed: 10696240.
- Heney N, Ahmed S, Flanagan M, et al. Superficial Bladder Cancer: Progression and Recurrence. *Journal of Urology*. 1983; 130(6): 1083–1086, doi: [10.1016/s0022-5347\(17\)51695-x](https://doi.org/10.1016/s0022-5347(17)51695-x).
- Althausen AF, Prout GR, Daly JJ. Non-invasive papillary carcinoma of the bladder associated with carcinoma *in situ*. *J Urol*. 1976; 116(5): 575–580, doi: [10.1016/s0022-5347\(17\)58916-8](https://doi.org/10.1016/s0022-5347(17)58916-8), indexed in Pubmed: 978809.

17. Kiemeny LA, Witjes JA, Heijbroek RP, et al. Dysplasia in normal-looking urothelium increases the risk of tumour progression in primary superficial bladder cancer. *Eur J Cancer*. 1994; 30A(11): 1621–1625, doi: [10.1016/0959-8049\(94\)e0133-o](https://doi.org/10.1016/0959-8049(94)e0133-o), indexed in Pubmed: [7833133](https://pubmed.ncbi.nlm.nih.gov/7833133/).
18. Lamm DL. Carcinoma *in situ*. *Urol Clin North Am*. 1992; 19(3): 499–508.
19. Lamm D. COMPLICATIONS OF BACILLUS CALMETTE-GUÉRIN IMMUNOTHERAPY. *Urol Clin North Am*. 1992; 19(3): 565–572, doi: [10.1016/s0094-0143\(21\)00423-7](https://doi.org/10.1016/s0094-0143(21)00423-7).
20. Amling CL. Diagnosis and management of superficial bladder cancer. *Curr Probl Cancer*. 2001; 25(4): 219–278, doi: [10.1067/mcn.2001.117539](https://doi.org/10.1067/mcn.2001.117539), indexed in Pubmed: [11514784](https://pubmed.ncbi.nlm.nih.gov/11514784/).
21. MELICOW MM. Histological study of vesical urothelium intervening between gross neoplasms in total cystectomy. *J Urol*. 1952; 68(1): 261–279, doi: [10.1016/s0022-5347\(17\)68193-x](https://doi.org/10.1016/s0022-5347(17)68193-x), indexed in Pubmed: [14939458](https://pubmed.ncbi.nlm.nih.gov/14939458/).
22. Hudson MA, Herr HW. Carcinoma *in situ* of the bladder. *J Urol*. 1995; 153(3 Pt 1): 564–572, doi: [10.1097/00005392-199503000-00002](https://doi.org/10.1097/00005392-199503000-00002), indexed in Pubmed: [7861485](https://pubmed.ncbi.nlm.nih.gov/7861485/).
23. Utz DC, Hanash KA, Farrow GM. The plight of the patient with carcinoma *in situ* of the bladder. *J Urol*. 1970; 103(2): 160–164, doi: [10.1016/s0022-5347\(17\)61913-x](https://doi.org/10.1016/s0022-5347(17)61913-x), indexed in Pubmed: [5410591](https://pubmed.ncbi.nlm.nih.gov/5410591/).
24. Sibony M, Billerey C. So-called "superficial" bladder tumors. Which classification. 2003; 23(1): 35–45.
25. Koss LG. Mapping of the urinary bladder: its impact on the concepts of bladder cancer. *Hum Pathol*. 1979; 10(5): 533–548, doi: [10.1016/s0046-8177\(79\)80097-0](https://doi.org/10.1016/s0046-8177(79)80097-0), indexed in Pubmed: [527959](https://pubmed.ncbi.nlm.nih.gov/527959/).
26. Melamed MR, Voutsas NG, Grabstald H, et al. NATURAL HISTORY AND CLINICAL BEHAVIOR OF *In situ* CARCINOMA OF THE HUMAN URINARY BLADDER. *Cancer*. 1964; 17(6): 1533–1545, doi: [10.1002/1097-0142\(196412\)17:12<1533::aid-cnrcr2820171205>3.0.co;2-7](https://doi.org/10.1002/1097-0142(196412)17:12<1533::aid-cnrcr2820171205>3.0.co;2-7), indexed in Pubmed: [14239679](https://pubmed.ncbi.nlm.nih.gov/14239679/).
27. Cheng L, Chevlieu JC, Neumann RM, et al. Survival of patients with carcinoma *in situ* of the urinary bladder. *Cancer*. 1999; 85(11): 2469–2474, indexed in Pubmed: [10357420](https://pubmed.ncbi.nlm.nih.gov/10357420/).
28. Oosterlinck W, Lobel B, Jackse G, et al. European Association of Urology, European Association of Urology (EAU) Working Group on Oncological Urology. Guidelines on bladder cancer. *Eur Urol*. 2002; 41(2): 105–112, doi: [10.1016/s0302-2838\(01\)00026-4](https://doi.org/10.1016/s0302-2838(01)00026-4), indexed in Pubmed: [12074395](https://pubmed.ncbi.nlm.nih.gov/12074395/).
29. Khatib SE. JLM, médecine U de NIF de. Interactions Lumière-Tissu Dans Le Diagnostic et Le Traitement Du Cancer de La Vessie. 2005. <https://books.google.com.lb/books?id=StHmGECAAJ>.
30. Bastacky S, Ibrahim S, Wilczynski SP, et al. The accuracy of urinary cytology in daily practice. *Cancer*. 1999; 87(3): 118–128, doi: [10.1002/\(sici\)1097-0142\(19990625\)87:3<118::aid-cnrcr4>3.0.co;2-n](https://doi.org/10.1002/(sici)1097-0142(19990625)87:3<118::aid-cnrcr4>3.0.co;2-n), indexed in Pubmed: [10385442](https://pubmed.ncbi.nlm.nih.gov/10385442/).
31. Kriegmair M, Baumgartner R, Lumper W, et al. Early clinical experience with 5-aminolevulinic acid for the photodynamic therapy of superficial bladder cancer. *Br J Urol*. 1996; 77(5): 667–671, doi: [10.1046/j.1464-410x.1996.09717.x](https://doi.org/10.1046/j.1464-410x.1996.09717.x), indexed in Pubmed: [8689107](https://pubmed.ncbi.nlm.nih.gov/8689107/).
32. Göğüş C, Bedük Y, Türkölmez K, et al. The significance of random bladder biopsies in superficial bladder cancer. *Int Urol Nephrol*. 2002; 34(1): 59–61, doi: [10.1023/a:1021354811825](https://doi.org/10.1023/a:1021354811825), indexed in Pubmed: [12549641](https://pubmed.ncbi.nlm.nih.gov/12549641/).
33. Herr HW. The value of a second transurethral resection in evaluating patients with bladder tumors. *J Urol*. 1999; 162(1): 74–76, doi: [10.1097/00005392-199907000-00018](https://doi.org/10.1097/00005392-199907000-00018), indexed in Pubmed: [10379743](https://pubmed.ncbi.nlm.nih.gov/10379743/).
34. Khatib SE, Leroux A, Merlin JL, et al. Photobleaching Kinetics and Epithelial Distribution of Hexylaminolevulinic Acid Induced PpIX in Rat Bladder Cancer. Conference: World Academy of Science, Engineering and Technology. 2016.
35. Nohara T, Kamijima T, Fukuda R, et al. Variations in photodynamic diagnosis for bladder cancer due to the quality of endoscopic equipment. *Photodiagnosis Photodyn Ther*. 2022; 37: 102628, doi: [10.1016/j.pdpdt.2021.102628](https://doi.org/10.1016/j.pdpdt.2021.102628), indexed in Pubmed: [34808397](https://pubmed.ncbi.nlm.nih.gov/34808397/).
36. Policard A. Etudes sur les aspects offerts par des tumeur experimentales examinee a la lumiere de woods. *CR Soc Biol*. 1924; 91(1423-1428): 241–256.
37. Auler H, Banzer G. Untersuchungen über die Rolle der Porphyrine bei geschwulstkranken Menschen und Tieren. *Zeitschrift für Krebsforschung*. 1942; 53(2): 65–68, doi: [10.1007/bf01792783](https://doi.org/10.1007/bf01792783).
38. FIGGE FHJ, WEILAND GS, MANGANIELLO LOJ. Cancer detection and therapy; affinity of neoplastic, embryonic, and traumatized tissues for porphyrins and metalloporphyrins. *Proc Soc Exp Biol Med*. 1948; 68(3): 640, doi: [10.3181/00379727-68-16580](https://doi.org/10.3181/00379727-68-16580), indexed in Pubmed: [18884315](https://pubmed.ncbi.nlm.nih.gov/18884315/).
39. LIPSON RL, BALDES EJ, OLSEN AM. The use of a derivative of hematoporphyrin in tumor detection. *J Natl Cancer Inst*. 1961; 26: 1–11, indexed in Pubmed: [13762612](https://pubmed.ncbi.nlm.nih.gov/13762612/).
40. Kelly JF, Snell ME. Hematoporphyrin derivative: a possible aid in the diagnosis and therapy of carcinoma of the bladder. *J Urol*. 1976; 115(2): 150–151, doi: [10.1016/s0022-5347\(17\)59108-9](https://doi.org/10.1016/s0022-5347(17)59108-9), indexed in Pubmed: [1249866](https://pubmed.ncbi.nlm.nih.gov/1249866/).
41. Benson Jr RC, Farrow GM, Kinsey JH, et al. Detection and localization of *In situ* carcinoma of the bladder with hematoporphyrin derivative. *Mayo Clin Proc*. 1982; 57(9): 548–555.
42. Windahl T, Peng Q, Moan J, et al. Uptake and distribution of intravenously or intravesically administered photosensitizers in the rat. *Cancer Lett*. 1993; 75(1): 65–70, doi: [10.1016/0304-3835\(93\)90209-r](https://doi.org/10.1016/0304-3835(93)90209-r), indexed in Pubmed: [8287383](https://pubmed.ncbi.nlm.nih.gov/8287383/).
43. Xiao Z, Miller GG, McCallum TJ, et al. Biodistribution of Photofrin II and 5-aminolevulinic acid-induced protoporphyrin IX in normal rat bladder and bladder tumor models: implications for photodynamic therapy. *Photochem Photobiol*. 1998; 67(5): 573–583, indexed in Pubmed: [9613241](https://pubmed.ncbi.nlm.nih.gov/9613241/).
44. Leveckis J, Burn JL, Brown NJ, et al. Kinetics of endogenous protoporphyrin IX induction by aminolevulinic acid: preliminary studies in the bladder. *J Urol*. 1994; 152(2 Pt 1): 550–553, doi: [10.1016/s0022-5347\(17\)32791-x](https://doi.org/10.1016/s0022-5347(17)32791-x), indexed in Pubmed: [8015110](https://pubmed.ncbi.nlm.nih.gov/8015110/).
45. Chang SC, Buonaccorsi G, MacRobert A, et al. 5-aminolevulinic acid (ALA)-induced protoporphyrin IX fluorescence and photodynamic effects in the rat bladder: An *in vivo* study comparing oral and intravesical ALA administration. *Lasers Surg Med*. 1997; 20(3): 254–264, doi: [10.1002/\(sici\)1096-9101\(1997\)20:3<254::aid-lsm4>3.0.co;2-p](https://doi.org/10.1002/(sici)1096-9101(1997)20:3<254::aid-lsm4>3.0.co;2-p).
46. Iinuma S, Bachor R, Flotte T, et al. Investigative Urology: Biodistribution and Phototoxicity of 5-Aminolevulinic Acid-Induced PpIX in an Orthotopic Rat Bladder Tumor Model. *Journal of Urology*. 1995; 153(3): 802–806, doi: [10.1016/s0022-5347\(01\)67726-7](https://doi.org/10.1016/s0022-5347(01)67726-7).
47. D'Hallewin MA, Vanherzeele H, Baert L. Fluorescence detection of flat transitional cell carcinoma after intravesical instillation of aminolevulinic acid. *Am J Clin Oncol*. 1998; 21(3): 223–225, doi: [10.1097/0000421-199806000-00002](https://doi.org/10.1097/0000421-199806000-00002), indexed in Pubmed: [9626785](https://pubmed.ncbi.nlm.nih.gov/9626785/).
48. Jichlinski P, Wagnieres G, Forrer M, et al. The clinical value of fluorescence cystoscopy in the detection of superficial transitional epithelial cell carcinoma of the bladder. *Ann Urol (Paris)*. 1997; 31(1): 43–48.
49. Koenig F, McGovern FJ, Larne R, et al. Diagnosis of bladder carcinoma using protoporphyrin IX fluorescence induced by 5-aminolevulinic acid. *BJU Int*. 1999; 83(1): 129–135, doi: [10.1046/j.1464-410x.1999.00917.x](https://doi.org/10.1046/j.1464-410x.1999.00917.x), indexed in Pubmed: [10233465](https://pubmed.ncbi.nlm.nih.gov/10233465/).
50. Kriegmair M, Baumgartner R, Knuechel R, et al. Fluorescence photodetection of neoplastic urothelial lesions following intravesical instillation of 5-aminolevulinic acid. *Urology*. 1994; 44(6): 836–841, doi: [10.1016/s0090-4295\(94\)80167-3](https://doi.org/10.1016/s0090-4295(94)80167-3), indexed in Pubmed: [7985312](https://pubmed.ncbi.nlm.nih.gov/7985312/).
51. Zaak D, Kriegmair M, Stepp H, et al. Endoscopic detection of transitional cell carcinoma with 5-aminolevulinic acid: results of 1012 fluorescence endoscopies. *Urology*. 2001; 57(4): 690–694, doi: [10.1016/s0090-4295\(00\)01053-0](https://doi.org/10.1016/s0090-4295(00)01053-0), indexed in Pubmed: [11306382](https://pubmed.ncbi.nlm.nih.gov/11306382/).
52. Kloek J, Akkermans W, Henegouwen G. Derivatives of 5-Aminolevulinic Acid for Photodynamic Therapy: Enzymatic Conversion into Protoporphyrin. *Photochemistry and Photobiology*. 1998; 67(1): 150–154, doi: [10.1111/j.1751-1097.1998.tb05178.x](https://doi.org/10.1111/j.1751-1097.1998.tb05178.x).
53. Kloek J, Akkermans W, Beijersbergen van Henegouwen GM, et al. Prodrugs of 5-aminolevulinic acid for photodynamic therapy. *Photochem Photobiol*. 1996; 64(6): 994–1000, doi: [10.1111/j.1751-1097.1996.tb01868.x](https://doi.org/10.1111/j.1751-1097.1996.tb01868.x), indexed in Pubmed: [8972644](https://pubmed.ncbi.nlm.nih.gov/8972644/).
54. Lange N, Jichlinski P, Zellweger M, et al. Photodetection of early human bladder cancer based on the fluorescence of 5-aminolevulinic acid hexylester-induced protoporphyrin IX: a pilot study. *Br J Cancer*. 1999; 80(1-2): 185–193, doi: [10.1038/sj.bjc.6690338](https://doi.org/10.1038/sj.bjc.6690338), indexed in Pubmed: [10389995](https://pubmed.ncbi.nlm.nih.gov/10389995/).
55. MARTI A, LANGE N, BERGH HV, et al. OPTIMISATION OF THE FORMATION AND DISTRIBUTION OF PROTOPORPHYRIN IX IN THE UROTHELIUM. *The Journal of Urology*. 1999; 546–552, doi: [10.1097/00005392-199908000-00085](https://doi.org/10.1097/00005392-199908000-00085).
56. D'Hallewin MA, De Witte PA, Waelkens E, et al. Fluorescence detection of flat bladder carcinoma *in situ* after intravesical instillation of hypericin. *J Urol*. 2000; 164(2): 349–351, indexed in Pubmed: [10893582](https://pubmed.ncbi.nlm.nih.gov/10893582/).
57. D'Hallewin MA, Kamuhabwa AR, Roskams T, et al. Hypericin-based fluorescence diagnosis of bladder carcinoma. *BJU Int*. 2002; 89(7): 760–763, doi: [10.1046/j.1464-410x.2002.02690.x](https://doi.org/10.1046/j.1464-410x.2002.02690.x), indexed in Pubmed: [11966641](https://pubmed.ncbi.nlm.nih.gov/11966641/).
58. Lavie G, Mazur Y, Lavie D, et al. The chemical and biological properties of hypericin—a compound with a broad spectrum of biological activities. *Med Res Rev*. 1995; 15(2): 111–119, doi: [10.1002/med.2610150203](https://doi.org/10.1002/med.2610150203), indexed in Pubmed: [7739292](https://pubmed.ncbi.nlm.nih.gov/7739292/).
59. Bochenek K, Aebischer D, Międzybrodzka A, et al. Methods for bladder cancer diagnosis - The role of autofluorescence and photodynamic diagnosis. *Photodiagnosis Photodyn Ther*. 2019; 27: 141–148, doi: [10.1016/j.pdpdt.2019.05.036](https://doi.org/10.1016/j.pdpdt.2019.05.036), indexed in Pubmed: [31152879](https://pubmed.ncbi.nlm.nih.gov/31152879/).
60. Alfano R, Tata D, Cordero J, et al. Laser induced fluorescence spectroscopy from native cancerous and normal tissue. *IEEE*

- Journal of Quantum Electronics. 1984; 20(12): 1507–1511, doi: [10.1109/jqe.1984.1072322](https://doi.org/10.1109/jqe.1984.1072322).
61. D'Hallewin MA, Baert L, Vanherzeele H. Fluorescence imaging of bladder cancer. *Acta Urol Belg*. 1994; 62(4): 49–52, indexed in Pubmed: [7793348](https://pubmed.ncbi.nlm.nih.gov/7793348/).
  62. Richards-Kortum R, Sevick-Muraca E. Quantitative optical spectroscopy for tissue diagnosis. *Annu Rev Phys Chem*. 1996; 47: 555–606, doi: [10.1146/annurev.physchem.47.1.555](https://doi.org/10.1146/annurev.physchem.47.1.555), indexed in Pubmed: [8930102](https://pubmed.ncbi.nlm.nih.gov/8930102/).
  63. Wagnières GA, Star WM, Wilson BC. In vivo fluorescence spectroscopy and imaging for oncological applications. *Photochem Photobiol*. 1998; 68(5): 603–632, indexed in Pubmed: [9825692](https://pubmed.ncbi.nlm.nih.gov/9825692/).
  64. Anidjar M, Cussenot O, Avrillier S, et al. Laser induced autofluorescence diagnosis of bladder tumors: dependence on the excitation wavelength. *J Urol*. 1996; 156(5): 1590–1596, indexed in Pubmed: [8863545](https://pubmed.ncbi.nlm.nih.gov/8863545/).
  65. Anidjar M, Cussenot O, Avrillier S, et al. The role of laser-induced autofluorescence spectroscopy in bladder tumor detection. Dependence on the excitation wavelength. *Ann N Y Acad Sci*. 1998; 838: 130–142, doi: [10.1111/j.1749-6632.1998.tb08194.x](https://doi.org/10.1111/j.1749-6632.1998.tb08194.x), indexed in Pubmed: [9511802](https://pubmed.ncbi.nlm.nih.gov/9511802/).
  66. Koenig F, McGovern FJ, Enquist H, et al. Autofluorescence guided biopsy for the early diagnosis of bladder carcinoma. *J Urol*. 1998; 159(6): 1871–1875, indexed in Pubmed: [9598478](https://pubmed.ncbi.nlm.nih.gov/9598478/).
  67. Koenig F, McGovern FJ, Althausen AF, et al. Laser induced autofluorescence diagnosis of bladder cancer. *J Urol*. 1996; 156(5): 1597–1601, indexed in Pubmed: [8863546](https://pubmed.ncbi.nlm.nih.gov/8863546/).
  68. Zaak D, Stepp H, Baumgartner R, et al. Ultraviolet-excited (308 nm) autofluorescence for bladder cancer detection. *Urology*. 2002; 60(6): 1029–1033, doi: [10.1016/s0090-4295\(02\)01999-4](https://doi.org/10.1016/s0090-4295(02)01999-4), indexed in Pubmed: [12475664](https://pubmed.ncbi.nlm.nih.gov/12475664/).
  69. Frimberger D, Zaak D, Stepp H, et al. Autofluorescence imaging to optimize 5-ALA-induced fluorescence endoscopy of bladder carcinoma. *Urology*. 2001; 58(3): 372–375, doi: [10.1016/s0090-4295\(01\)01222-5](https://doi.org/10.1016/s0090-4295(01)01222-5), indexed in Pubmed: [11549483](https://pubmed.ncbi.nlm.nih.gov/11549483/).
  70. De Dominicis C, Liberti M, Perugia G, et al. Role of 5-aminolevulinic acid in the diagnosis and treatment of superficial bladder cancer: improvement in diagnostic sensitivity. *Urology*. 2001; 57(6): 1059–1062, doi: [10.1016/s0090-4295\(01\)00948-7](https://doi.org/10.1016/s0090-4295(01)00948-7), indexed in Pubmed: [11377304](https://pubmed.ncbi.nlm.nih.gov/11377304/).
  71. Filbeck T, Pichlmeier U, Kneuchel R, et al. Do patients profit from 5-aminolevulinic acid-induced fluorescence diagnosis in transurethral resection of bladder carcinoma? *Urology*. 2002; 60(6): 1025–1028, doi: [10.1016/s0090-4295\(02\)01961-1](https://doi.org/10.1016/s0090-4295(02)01961-1), indexed in Pubmed: [12475663](https://pubmed.ncbi.nlm.nih.gov/12475663/).
  72. Jichlinski P, Wagnières G, Forrer M, et al. Clinical assessment of fluorescence cystoscopy during transurethral bladder resection in superficial bladder cancer. *Urological Research*. 1997; 25(S1): S3–S6, doi: [10.1007/bf00942040](https://doi.org/10.1007/bf00942040).
  73. Filbeck T, Roessler W, Kneuchel R, et al. 5-aminolevulinic acid-induced fluorescence endoscopy applied at secondary transurethral resection after conventional resection of primary superficial bladder tumors. *Urology*. 1999; 53(1): 77–81, doi: [10.1016/s0090-4295\(98\)00430-0](https://doi.org/10.1016/s0090-4295(98)00430-0), indexed in Pubmed: [9886592](https://pubmed.ncbi.nlm.nih.gov/9886592/).
  74. Grimbergen M, Swol Cv, Jonges T, et al. Reduced Specificity of 5-ALA Induced Fluorescence in Photodynamic Diagnosis of Transitional Cell Carcinoma after Previous Intravesical Therapy. *European Urology*. 2003; 44(1): 51–56, doi: [10.1016/s0302-2838\(03\)00210-0](https://doi.org/10.1016/s0302-2838(03)00210-0).
  75. Hartmann A, Moser K, Kriegsmair M, et al. Frequent genetic alterations in simple urothelial hyperplasias of the bladder in patients with papillary urothelial carcinoma. *Am J Pathol*. 1999; 154(3): 721–727, doi: [10.1016/S0002-9440\(10\)65318-7](https://doi.org/10.1016/S0002-9440(10)65318-7), indexed in Pubmed: [10079249](https://pubmed.ncbi.nlm.nih.gov/10079249/).
  76. Riedl CR, Danilchenko D, Koenig F, et al. Fluorescence endoscopy with 5-aminolevulinic acid reduces early recurrence rate in superficial bladder cancer. *J Urol*. 2001; 165(4): 1121–1123, indexed in Pubmed: [11257651](https://pubmed.ncbi.nlm.nih.gov/11257651/).
  77. Jichlinski P, Guillou L, Karlsen SJ, et al. Hexyl aminolevulinic acid fluorescence cystoscopy: new diagnostic tool for photodiagnosis of superficial bladder cancer—a multicenter study. *J Urol*. 2003; 170(1): 226–229, doi: [10.1097/01.ju.0000060782.52358.04](https://doi.org/10.1097/01.ju.0000060782.52358.04), indexed in Pubmed: [12796694](https://pubmed.ncbi.nlm.nih.gov/12796694/).
  78. Schmidbauer J, Witjes F, Schmeller N, et al. Hexvix PCB301/01 Study Group. Improved detection of urothelial carcinoma *in situ* with hexaminolevulinic acid fluorescence cystoscopy. *J Urol*. 2004; 171(1): 135–138, doi: [10.1097/01.ju.0000100480.70769.0e](https://doi.org/10.1097/01.ju.0000100480.70769.0e), indexed in Pubmed: [14665861](https://pubmed.ncbi.nlm.nih.gov/14665861/).
  79. Marti A, Jichlinski P, Lange N, et al. Comparison of aminolevulinic acid and hexylester aminolevulinic acid induced protoporphyrin IX distribution in human bladder cancer. *J Urol*. 2003; 170(2 Pt 1): 428–432, doi: [10.1097/01.ju.0000075054.38441.2d](https://doi.org/10.1097/01.ju.0000075054.38441.2d), indexed in Pubmed: [12853792](https://pubmed.ncbi.nlm.nih.gov/12853792/).
  80. D'Hallewin MA, El Khatib S, Leroux A, et al. Endoscopic confocal fluorescence microscopy of normal and tumor bearing rat bladder. *J Urol*. 2005; 174(2): 736–740, doi: [10.1097/01.ju.0000164729.36663.8d](https://doi.org/10.1097/01.ju.0000164729.36663.8d), indexed in Pubmed: [16006967](https://pubmed.ncbi.nlm.nih.gov/16006967/).
  81. Chan KM, Gleadle J, Li J, et al. Improving hexaminolevulinic acid enabled cancer cell detection in liquid biopsy immunosensors. *Sci Rep*. 2021; 11(1): 7283, doi: [10.1038/s41598-021-86649-6](https://doi.org/10.1038/s41598-021-86649-6), indexed in Pubmed: [33790357](https://pubmed.ncbi.nlm.nih.gov/33790357/).
  82. Sim HG, Lau WKO, Olivo M, et al. Is photodynamic diagnosis using hypericin better than white-light cystoscopy for detecting superficial bladder carcinoma? *BJU Int*. 2005; 95(9): 1215–1218, doi: [10.1111/j.1464-410X.2005.05508.x](https://doi.org/10.1111/j.1464-410X.2005.05508.x), indexed in Pubmed: [15892804](https://pubmed.ncbi.nlm.nih.gov/15892804/).
  83. Pytel A, Schmeller N. New aspect of photodynamic diagnosis of bladder tumors: fluorescence cytology. *Urology*. 2002; 59(2): 216–219, doi: [10.1016/s0090-4295\(01\)01528-x](https://doi.org/10.1016/s0090-4295(01)01528-x), indexed in Pubmed: [11834388](https://pubmed.ncbi.nlm.nih.gov/11834388/).
  84. Tauber S, Schneede P, Liedl B, et al. Fluorescence cytology of the urinary bladder. *Urology*. 2003; 61(5): 1067–1071, doi: [10.1016/s0090-4295\(02\)02554-2](https://doi.org/10.1016/s0090-4295(02)02554-2).
  85. Olivo M, Lau W, Manivasager V, et al. Novel photodynamic diagnosis of bladder cancer: ex vivo fluorescence cytology using hypericin. *Int J Oncol*. 2003; 23(6): 1501–1504, indexed in Pubmed: [14612919](https://pubmed.ncbi.nlm.nih.gov/14612919/).
  86. Koenig F, Knittel J, Stepp H. Diagnosing cancer *in vivo*. *Science*. 2001; 292(5520): 1401–1403, doi: [10.1126/science.292.5520.1401](https://doi.org/10.1126/science.292.5520.1401), indexed in Pubmed: [11360991](https://pubmed.ncbi.nlm.nih.gov/11360991/).
  87. Wang TD, Van Dam J. Optical biopsy: a new frontier in endoscopic detection and diagnosis. *Clin Gastroenterol Hepatol*. 2004; 2(9): 744–753, indexed in Pubmed: [15354274](https://pubmed.ncbi.nlm.nih.gov/15354274/).
  88. Wu J, Wang YC, Luo WJ, et al. Diagnostic Performance of Confocal Laser Endomicroscopy for the Detection of Bladder Cancer: Systematic Review and Meta-Analysis. *Urol Int*. 2020; 104(7-8): 523–532, doi: [10.1159/000508417](https://doi.org/10.1159/000508417), indexed in Pubmed: [32554957](https://pubmed.ncbi.nlm.nih.gov/32554957/).
  89. Chalau V, Didelon J, Istomin J, et al. IN VIVO CANCER DIAGNOSTICS BY SPACE RESOLVED DIFFUSE REFLECTANCE SPECTROSCOPY. *Diagnostic Optical Spectroscopy in Biomedicine II*. 2003, doi: [10.1364/ecbo.2003.5141\\_333](https://doi.org/10.1364/ecbo.2003.5141_333).
  90. Mourant JR, Bigio IJ, Boyer J, et al. Spectroscopic diagnosis of bladder cancer with elastic light scattering. *Lasers Surg Med*. 1995; 17(4): 350–357, doi: [10.1002/ism.1900170403](https://doi.org/10.1002/ism.1900170403), indexed in Pubmed: [8684237](https://pubmed.ncbi.nlm.nih.gov/8684237/).
  91. Crow P, Molckovsky A, Stone N, et al. Assessment of fiberoptic near-infrared raman spectroscopy for diagnosis of bladder and prostate cancer. *Urology*. 2005; 65(6): 1126–1130, doi: [10.1016/j.urology.2004.12.058](https://doi.org/10.1016/j.urology.2004.12.058), indexed in Pubmed: [15913721](https://pubmed.ncbi.nlm.nih.gov/15913721/).
  92. Guillemain F, A'Amar O, Rezzoug H, et al. Optical instrumentation suitable for a real-time dosimetry during photodynamic therapy. *SPIE Proceedings*. 1995, doi: [10.1117/12.228879](https://doi.org/10.1117/12.228879).
  93. Jesser CA, Boppart SA, Pitris C, et al. High resolution imaging of transitional cell carcinoma with optical coherence tomography: feasibility for the evaluation of bladder pathology. *Br J Radiol*. 1999; 72(864): 1170–1176, doi: [10.1259/bjr.72.864.10703474](https://doi.org/10.1259/bjr.72.864.10703474), indexed in Pubmed: [10703474](https://pubmed.ncbi.nlm.nih.gov/10703474/).
  94. Tearney GJ, Brezinski ME, Southern JF, et al. Optical biopsy in human urologic tissue using optical coherence tomography. *J Urol*. 1997; 157(5): 1915–1919, indexed in Pubmed: [9112562](https://pubmed.ncbi.nlm.nih.gov/9112562/).
  95. Xie T, Xie H, Fedder GK, et al. Endoscopic optical coherence tomography with a modified microelectromechanical systems mirror for detection of bladder cancers. *Appl Opt*. 2003; 42(31): 6422–6426, doi: [10.1364/ao.42.006422](https://doi.org/10.1364/ao.42.006422), indexed in Pubmed: [14649286](https://pubmed.ncbi.nlm.nih.gov/14649286/).
  96. Zagaynova EV, Streltsova OS, Gladkova ND, et al. In vivo optical coherence tomography feasibility for bladder disease. *J Urol*. 2002; 167(3): 1492–1496, indexed in Pubmed: [11832776](https://pubmed.ncbi.nlm.nih.gov/11832776/).
  97. MacAulay C, Lane P, Richards-Kortum R. In vivo pathology: microendoscopy as a new endoscopic imaging modality. *Gastrointest Endosc Clin N Am*. 2004; 14(3): 595–620, xi, doi: [10.1016/j.giec.2004.03.014](https://doi.org/10.1016/j.giec.2004.03.014), indexed in Pubmed: [15261205](https://pubmed.ncbi.nlm.nih.gov/15261205/).
  98. Vieller B, Genet M, Berier F. Confocal Imaging Equipement in Particular for Endoscope. , France 2002.
  99. Wu J, Wang YC, Dai Bo, et al. Optical biopsy of bladder cancer using confocal laser endomicroscopy. *Int Urol Nephrol*. 2019; 51(9): 1473–1479, doi: [10.1007/s11255-019-02197-z](https://doi.org/10.1007/s11255-019-02197-z), indexed in Pubmed: [31214952](https://pubmed.ncbi.nlm.nih.gov/31214952/).
  100. von Rundstedt FC, Lerner SP. New imaging techniques for nonmuscle invasive bladder cancer. *Curr Opin Urol*. 2014; 24(5): 532–539, doi: [10.1097/MOU.0000000000000093](https://doi.org/10.1097/MOU.0000000000000093), indexed in Pubmed: [25051025](https://pubmed.ncbi.nlm.nih.gov/25051025/).
  101. Lerner S, Goh A. Novel endoscopic diagnosis for bladder cancer. *Cancer*. 2014; 121(2): 169–178, doi: [10.1002/cncr.28905](https://doi.org/10.1002/cncr.28905).
  102. Tadrous P. Methods for imaging the structure and function of living tissues and cells: 3. Confocal microscopy and micro-radiology. *The Journal of Pathology*. 2000; 191(4): 345–354, doi: [10.1002/1096-9896\(200008\)191:4<345::aid-path696>3.0.co;2-r](https://doi.org/10.1002/1096-9896(200008)191:4<345::aid-path696>3.0.co;2-r).
  103. Koenig F, Knittel J, Schnieder L, et al. Confocal laser scanning microscopy of urinary bladder after intravesical instillation of a fluorescent dye. *Urology*. 2003; 62(1): 158–161, doi: [10.1016/s0090-4295\(03\)00121-3](https://doi.org/10.1016/s0090-4295(03)00121-3), indexed in Pubmed: [12837458](https://pubmed.ncbi.nlm.nih.gov/12837458/).

104. George M, Meining A. Cresyl violet as a fluorophore in confocal laser scanning microscopy for future in-vivo histopathology. *Endoscopy*. 2003; 35(7): 585–589, doi: [10.1055/s-2003-40245](https://doi.org/10.1055/s-2003-40245), indexed in Pubmed: [12822093](https://pubmed.ncbi.nlm.nih.gov/12822093/).
105. Swindle LD, Thomas SG, Freeman M, et al. View of normal human skin in vivo as observed using fluorescent fiber-optic confocal microscopic imaging. *J Invest Dermatol*. 2003; 121(4): 706–712, doi: [10.1046/j.1523-1747.2003.12477.x](https://doi.org/10.1046/j.1523-1747.2003.12477.x), indexed in Pubmed: [14632185](https://pubmed.ncbi.nlm.nih.gov/14632185/).
106. Anikijenko P, Vo LT, Murr ER, et al. In vivo detection of small sub-surface melanomas in athymic mice using noninvasive fiber optic confocal imaging. *J Invest Dermatol*. 2001; 117(6): 1442–1448, doi: [10.1046/j.0022-202x.2001.01592.x](https://doi.org/10.1046/j.0022-202x.2001.01592.x), indexed in Pubmed: [11886506](https://pubmed.ncbi.nlm.nih.gov/11886506/).
107. Breda A, Territo A, Guttilla A, et al. Correlation Between Confocal Laser Endomicroscopy (Cellvizio) and Histological Grading of Upper Tract Urothelial Carcinoma: A Step Forward for a Better Selection of Patients Suitable for Conservative Management. *Eur Urol Focus*. 2018; 4(6): 954–959, doi: [10.1016/j.euf.2017.05.008](https://doi.org/10.1016/j.euf.2017.05.008), indexed in Pubmed: [28753800](https://pubmed.ncbi.nlm.nih.gov/28753800/).
108. Al-Mansour MR, Caycedo-Marulanda A, Davis BR, et al. SAGES TAVAC safety and efficacy analysis confocal laser endomicroscopy. *Surg Endosc*. 2021; 35(5): 2091–2103, doi: [10.1007/s00464-020-07607-3](https://doi.org/10.1007/s00464-020-07607-3), indexed in Pubmed: [32405892](https://pubmed.ncbi.nlm.nih.gov/32405892/).
109. Laemmel E, Genet M, Le Goualher G, et al. Fibered confocal fluorescence microscopy (Cell-viZio) facilitates extended imaging in the field of microcirculation. A comparison with intravital microscopy. *J Vasc Res*. 2004; 41(5): 400–411, doi: [10.1159/000081209](https://doi.org/10.1159/000081209), indexed in Pubmed: [15467299](https://pubmed.ncbi.nlm.nih.gov/15467299/).
110. Rouse AR, Kano A, Udovich JA, et al. Design and demonstration of a miniature catheter for a confocal microendoscope. *Appl Opt*. 2004; 43(31): 5763–5771, doi: [10.1364/ao.43.005763](https://doi.org/10.1364/ao.43.005763), indexed in Pubmed: [15540433](https://pubmed.ncbi.nlm.nih.gov/15540433/).
111. Clark AL, Gillenwater AM, Collier TG, et al. Confocal microscopy for real-time detection of oral cavity neoplasia. *Clin Cancer Res*. 2003; 9(13): 4714–4721, indexed in Pubmed: [14581341](https://pubmed.ncbi.nlm.nih.gov/14581341/).
112. White WM, Baldassano M, Rajadhyaksha M, et al. Confocal reflectance imaging of head and neck surgical specimens. A comparison with histologic analysis. *Arch Otolaryngol Head Neck Surg*. 2004; 130(8): 923–928, doi: [10.1001/archotol.130.8.923](https://doi.org/10.1001/archotol.130.8.923), indexed in Pubmed: [15313861](https://pubmed.ncbi.nlm.nih.gov/15313861/).
113. Sung KB, Richards-Kortum R, Follen M, et al. Fiber optic confocal reflectance microscopy: a new real-time technique to view nuclear morphology in cervical squamous epithelium in vivo. *Optics Express*. 2003; 11(24): 3171, doi: [10.1364/oe.11.003171](https://doi.org/10.1364/oe.11.003171).
114. Liem EI, Freund JE, Savci-Hejjink CD, et al. Validation of Confocal Laser Endomicroscopy Features of Bladder Cancer: The Next Step Towards Real-time Histologic Grading. *Eur Urol Focus*. 2020; 6(1): 81–87, doi: [10.1016/j.euf.2018.07.012](https://doi.org/10.1016/j.euf.2018.07.012), indexed in Pubmed: [30033066](https://pubmed.ncbi.nlm.nih.gov/30033066/).
115. Marien A, Rock A, Maadarani KEI, et al. Urothelial Tumors and Dual-Band Imaging: A New Concept in Confocal Laser Endomicroscopy. *J Endourol*. 2017; 31(5): 538–544, doi: [10.1089/end.2016.0892](https://doi.org/10.1089/end.2016.0892), indexed in Pubmed: [28326794](https://pubmed.ncbi.nlm.nih.gov/28326794/).